Transport properties of the Au_{32} cluster with fullerene symmetry

Xiaohong Zheng, Xingqiang Shi, Zhenxiang Dai, and Zhi Zeng*
Key Laboratory of Materials Physics, Institute of Solid State Physics, Chinese Academy of Sciences, Hefei 230031, People's Republic of China

(Received 15 January 2006; revised manuscript received 20 July 2006; published 25 August 2006)

Nonequilibrium Green's function method combined with density functional theory is adopted to investigate the transport properties of an Au_{32} based device by an Au(100)-Au_{32}-Au(100) model, where the Au_{32} cluster has the same symmetry as that of C_{60}. The effects of the contact geometry and gate voltage on the conductance are studied. In contrast with the case of the C_{60} based device in which the charge transfer gives good conductivity, the high equilibrium conductance of the Au_{32} based device is found to originate from the mixing of the LUMO (lowest unoccupied molecular orbital) of the cluster and the electrode-induced gap state appearing in the HOMO (highest occupied molecular orbital)-LUMO gap. The *I-V* characteristics, and especially, the NDR (negative differential resistance) behavior in it can be understood by a rigid shift model of the HOMO-filtered energy region and LUMO-filtered energy region in the left and right electrodes under various biases.

DOI: 10.1103/PhysRevB.74.085418 PACS number(s): 85.65.+h, 73.63.−b, 36.40.−c

I. INTRODUCTION

The study of transport properties of molecular conductors in which molecules and clusters act as the key part has initiated extensive interest during the past several years both theoretically and experimentally since it is believed that they will play very important roles in future electronic circuits.[1,2] Many interesting phenomena have been observed in molecular conductors, such as highly nonlinear *I-V* characteristics, negative differential conductance, and electrical switching, etc. Among the systems that have been studied, carbon nanotubes and C_{60} have received the most attention since they are the most prospective building blocks in the realization of practical molecular conductors.[3–7] In particular, Taylor *et al.*'s theoretical work gives a 2.2 G_0 ($G_0=\frac{2e^2}{h}$, conductance quantum) conductance for C_{60} sandwiched between two Al(100) electrodes.[8] Obviously, the search for other stable clusters that can be used to construct molecular conductors and the study of the transport properties of them are still quite necessary.

In the study of cluster science, the search for other fullerene structures composed of noncarbon elements, especially of metal elements has been tried and never stopped since the discovery of C_{60} and *C* nanotubes. Much to our encouragement, many important discoveries have been reported in recent years. Au nanotubes, Pt nanotubes, and Si nanotubes have been fabricated or proved to exist successively.[9–12] In 2003, Li *et al.* reported a tetrahedral cluster Au_{20} with a hollow structure.[13] The energy gap of 1.77 eV means that it is a stable cluster. In 2004, two groups predicted the existence of an Au_{32} cluster with a fullerene (cagelike) structure almost simultaneously.[14,15] Au_{32} has the same symmetry, namely, I_h group, as that of C_{60}. The newest discovery shows that the energy of this structure is much lower than that of any other isomers with a solid structure. It is well known that there are twenty hexagons and twelve pentagons on the surface of C_{60}. Interestingly, Au_{32} can be constructed with C_{60} as a template. If an Au atom is placed at the center of each hexagon and each pentagon on the surface of C_{60} and then the *C* atoms are taken away, the left Au atoms form the hollow I_h structure of Au_{32}. The surface of the Au_{32} cluster is composed of twenty identical isosceles triangles, and Johansson *et al.*'s work[14] shows that the length of the equal sides of these isosceles triangles is 2.762 Å and the length of the third side 2.868 Å. The diameter of the sphere is 9.0 Å.

Although an Au_{32} cluster with a cagelike structure has not been fabricated experimentally, theoretical predictions are greatly helpful in searching for it in future experiments. And the physical properties of such a new structure are naturally worthy of being carefully studied. Actually, the optical properties of Au_{32} have been reported theoretically very recently.[16] In particular, stimulated by the study of C_{60}, the transport properties of Au_{32} have attracted our attention greatly. Therefore, in this work, the nonequilibrium Green's function method based on density-functional theory is adopted to investigate the transport properties of such a metal fullerene cluster Au_{32} which is sandwiched between two Au(100) electrodes with finite cross section. We find that its equilibrium conductance depends strongly on the distance between the cluster and the electrodes as well as the magnitude of gate voltages. Different from the case of C_{60} in which the charge transfer causes its good conductivity, the high equilibrium conductance of Au_{32} is found to originate from the mixing of the lowest unoccupied molecular orbital (LUMO) of the cluster and the electrode-induced gap state appearing in the highest occupied molecular orbital (HOMO)-LUMO gap. The *I-V* characteristics and negative differential resistance (NDR) in this device can be understood by a rigid shift model of the HOMO-filtered energy region (HFER) and LUMO-filtered energy region (LFER) in the left and right electrodes under various biases.

This paper is organized as follows: In Sec. II we give a brief description of the computational method and the simulation model. In Sec. III the main results and discussions are presented. A short conclusion is given in Sec. IV.

II. COMPUTATIONAL METHOD AND SIMULATION MODEL

Our investigation is based on a recently developed self-consistent first-principles technique which combines the

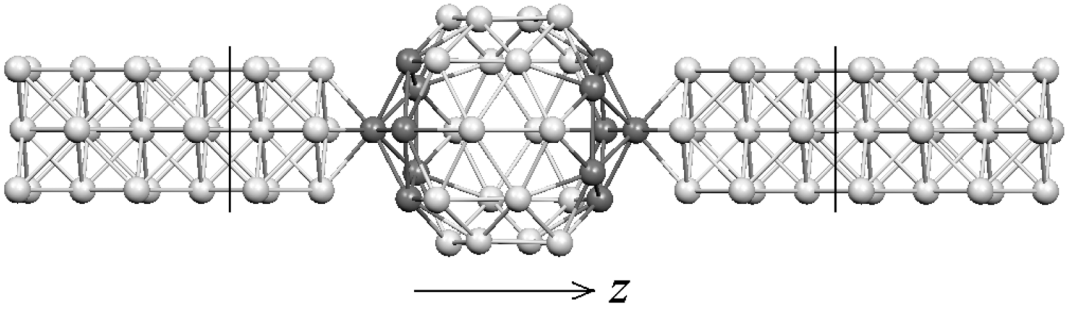

FIG. 1. The model structure of the device: a cagelike Au_{32} cluster is sandwiched between two Au(100) electrodes with finite cross section. The part between the two vertical lines is the extended molecule or the central region. The atoms of the two pentagons of the Au_{32} which are nearest to the electrodes are in black as a guide to the eyes. However, the atoms both in white and in black are gold.

Keldysh nonequilibrium Green's-function formalism (NEGF) with a self-consistent density-functional theory (DFT).[17–19] The package we use is the TranSIESTA-C, which incorporates the NEGF technique into the well tested SIESTA method[20] to realize the simulation of electrical transport in molecular conductors under nonequilibrium situations. The technical aspects of this method have been presented in great detail in Refs. 17 and 18 and the interested readers are referred to them.

The model structure we study is constructed as follows: we put the Au_{32} cluster between two Au(100) electrodes with a finite cross section. A large enough vacuum layer (with thickness of 32 Å) around the electrode in the x and y directions is chosen so that the device has no interaction with its mirror images. The electrodes are extacted from bulk gold and the number of atoms in each atomic layer along the z direction is arranged as 5,4,5,4…, as done by many authors.[8,21–24] Two surface layers (5,4) of the left electrode and three surface layers (4,5,4) of the right electrode together with the Au_{32} cluster are chosen as the central region, as shown in Fig. 1. Four layers (5,4,5,4) are chosen as the electrode cell for both the left and the right electrodes, which can satisfy the requirement that nonzero Hamiltonian matrix elements and overlap matrix elements only exist between the basis orbitals of atoms in the nearest electrode cells. Thus an electrode unit cell contains 18 Au atoms. To reflect the possible various contact geometries in a real situation when the cluster is sandwiched between the electrodes, we will consider the effects of the distance between the cluster and the electrodes as well as the relative orientation of the cluster to the electrodes on the equilibrium conductance. Meanwhile, the effects of the gate voltages which can modulate the electronic structure of the cluster are also considered. Finally, I-V characteristics are studied when the system is driven out of equilibrium by a bias voltage. Before the Au_{32} cluster is put between the electrodes, the structure and the stability of the cluster is reinvestigated with TranSIESTA-C package. The structure relaxation of the cluster shows negligible difference from Johansson's results.[14] We have also studied the stability of its cage structure when it is put between the electrodes, and found that the cage structure is still kept although it is elongated a bit along the direction of the electrodes. However, a fixed structure with I_h symmetry is used in our study and we do not take into account the structure changes induced by the bias voltage.[25]

III. RESULTS AND DISCUSSIONS

The transport properties of a molecular conductor strongly depend on the coupling between the molecule and the electrodes. And this coupling is determined by many factors such as the contact geometry, the band structure of the electrodes, and the electronic structure of the central molecule. In particular, the distance between the molecule and the electrodes as well as the gate voltages applied to the central molecule may greatly affect the transport behaviors of molecular conductors. Therefore, we will study the effects of these two factors on the equilibrium conductance of an Au_{32} cluster. Meanwhile, its nonequilibrium properties, namely, the I-V characteristics, will also be observed when it is driven out of equilibrium by bias voltages.

A. Equilibrium conductance

1. The effects of the contact geometry

In experiments, it is very difficult to determine the microstructure of the contact geometry of the molecular conductors, i.e., we do not exactly know what is the distance between the molecule and the electrodes and what is the orientation of the molecule relative to the electrodes when a molecule is sandwiched between two electrodes. However, in theoretical study, we can simulate all kinds of possible contact geometries by changing the distance and the relative orientation of the molecule. Among all the possible relative orientations of Au_{32}, one typical configuration is selected to inspect the distance effects on the conductance of Au_{32} cluster (shown in Fig. 1), in which the central axis of the electrodes (z axis) is arranged to coincide with the symmetry axis of the pentagonal pyramids at the two ends of the Au_{32} cluster.

The distance dependence of the equilibrium conductance (G-d curve) is shown in Fig. 2. It can be seen that the conductance does not vary monotonously with the distance. Instead, a peak appears and the conductance maximum (G_{max}) of 2.26 G_0 occurs at d=2.165 Å, which is comparable to the conductance of C_{60} (2.2 G_0).[8] This means that Au_{32} is a good conductor. It will be interesting to see whether the distance with G_{max} is exactly the equilibrium distance between the cluster and the electrodes. However, our study on the energetics of the system with varying distances shows that the equilibrium distance is 1.775 Å with the corresponding equi-

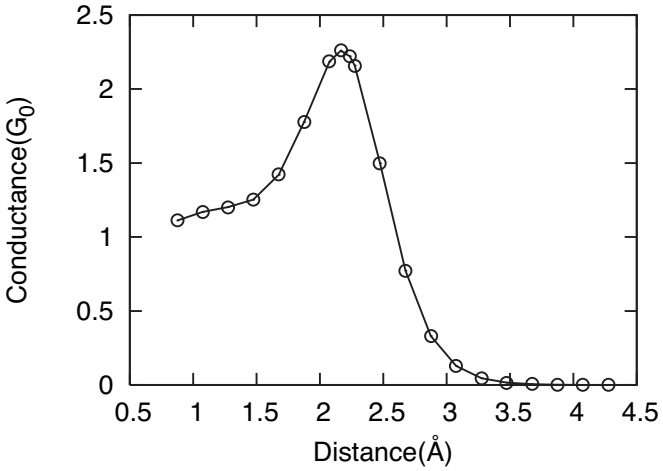

FIG. 2. The *G-d* curve: the effects of the distance on the equilibrium conductance.

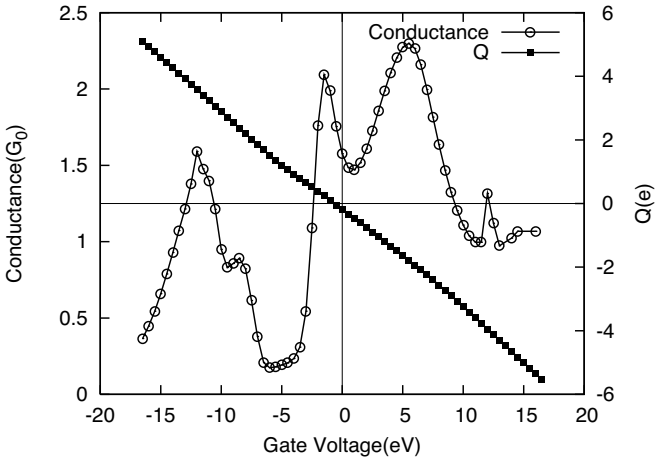

FIG. 3. The effects of the gate voltage (V_g) on the equilibrium conductance (G) and excess electrons (Q) on the Au_{32} cluster.

librium conductance of 1.57 G_0. This is not difficult to understand since the system might be at the lowest energy with some distance, but such a distance is not necessarily the most beneficial for the transmission of electrons. The transmission depends on the cooperation of many factors, such as the broadening of the energy levels of the central cluster, the alignment of the Fermi level of the electrodes within the HOMO-LUMO gap, charge transfer between the electrodes and the central cluster, localization of the molecular orbitals of the central cluster, as well as the overlap and matching of the electrode states and molecular states, etc. The variation of the distance may induce complicated changes of all these factors and reasonably causes the G_{max} not to appear at the equilibrium distance.

It is worthy of study as to why Au_{32} has a high conductance since its HOMO-LUMO gap is very large (about 1.71 eV in our calculation). For comparison, we would like to mention the C_{60} case first. The 1.77 eV HOMO-LUMO gap of C_{60} determines that the C_{60} molecular solid is a semiconductor but it can be doped up to six electrons since its LUMO is threefold degenerate and it conducts best when it is doped three electrons per C_{60} (Ref. 26). Taylor *et al.* found that it also conducts very well when it is sandwiched between two electrodes since the open electrodes provide a natural electron contributor (three electrons go from the electrodes to the cluster).[8] Therefore, it is the charge transfer that causes the high conductance of the C_{60} based molecular conductors. Does charge transfer also bring the high conductance of the Au_{32} based device? Our Mulliken population analysis shows that the charge transfer between the Au_{32} cluster and the electrodes is negligible (only 0.2 *e*, see the Q value at V_g=0 in Fig. 3) and thus the high conductivity of Au_{32} is not brought about by the charge transfer. It is easy to understand why there are three electrons from the Al electrodes to the C_{60} cluster while negligible electrons from the Au electrode to the Au_{32} cluster: the big difference between the work function of the Al electrodes (4.2 eV) and the central C_{60} cluster [11.7 eV (Ref. 27)] makes charge transfer much easier in the Al-C_{60}-Al device, while the difference of the work function of the electrodes and the central cluster is quite small in the Au-Au_{32}-Au device since all the components are of the same material. To gain insight into its conduction mechanism, the energy levels of the isolated cluster and the renormalized molecular levels[21] when it is sandwiched between the electrodes for the case with cluster-electrode distance d=1.775 Å are calculated and the levels around the Fermi energy are shown in Table I. From this table, we find that the fourfold degeneracy of the HOMO and LUMO is broken when the cluster is sandwiched between the electrodes and the HOMO-LUMO gap is reduced to 1.558 eV, a 0.15 eV reduction compared to the isolated cluster. However, both the renormalized HOMO and LUMO are far away from the Fermi level of the electrodes. It is interesting to notice that there is an isolated level in the HOMO-LUMO gap at −0.046 eV which is very close to the Fermi energy of the electrodes. This level is an electrode-induced gap state arising from the hybridization of gold surface states and occupied molecular states.[28,29] It is the broadening and mixing of this gap state with the broadened LUMO of the Au_{32} that causes such a high equilibrium conductance.

Another factor about the microstructure of the contact geometry is the orientation of the cluster relative to the

TABLE I. The molecular levels of the isolated Au_{32} and the renormalized molecular levels when it is sandwiched between the electrodes. In the sandwiched case, the energy is relative to the Fermi energy of the electrodes.

	Isolated(eV)	Sandwiched(eV)
HOMO_4	0.0	−1.068
HOMO_3	0.0	−1.068
HOMO_2	0.0	−0.879
HOMO_1	0.0	−0.873
		−0.046
LUMO_1	1.705	0.685
LUMO_2	1.705	0.686
LUMO_3	1.705	0.819
LUMO_4	1.705	0.820

electrodes.[23] We take this factor into account by rotating the Au_{32} cluster between the fixed electrodes. It is found that, due to the three-dimensional and spherelike structure of Au_{32}, there is not much difference among the conductances of all the possible cases with different orientations to the electrodes. In comparison, the effect of the relative orientation in this device is much weaker than that in the case of a planer Si_4 cluster where the equilibrium conductance is greatly affected by the relative orientation.[23]

2. The effects of the gate voltage

For a molecular conductor, its transport properties depend not only on the microstructure of the contact geometry, but also on the internal electronic states of the central cluster. For example, the current through C_{60} can be remarkably strengthened by a scanning tunnel microscope (STM) tip squeezing the cluster so as to change the alignment of the energy levels of the C_{60} to the Fermi level of the electrodes.[30] With this method, an electromechanical amplifier using a single molecule can be constructed. Another simple and direct way to modulate the internal states of the central cluster is to apply a gate voltage V_g to it,[8,24] which is the basis of a single molecular transistor. In the current version of TranSIESTA-C, the gate electrode is simulated simply by shifting the MPSH (molecular projected self-consistent Hamiltonian[21]), i.e., by raising or lowering the renormalized molecular levels of the cluster.

We take the case of Fig. 1 as an example to study the effects of gate voltage where the distance between the cluster and electrodes is taken as 1.775 Å. In particular, the variation of the conductance and the excess charge on the cluster are shown in Fig. 3. We find that excess charge on the cluster changes almost linearly with the gate voltage and the excess charge at $V_g=0$ is negligible, which means that charge transfer is not the key factor that determines the high conductance of this Au_{32} based device, as mentioned earlier. In contrast, an oscillating behavior of the equilibrium conductance is clearly observed in this figure. This phenomenon is closely related to the change of the alignment of the energy levels of the Au_{32} cluster to the Fermi level of the electrodes with the application of different gate voltages. For example, the peaks under −5 eV are from the HOMO levels, the peaks above 0 eV are from the LUMO levels, and the peak near 0 eV is due to the gap state (in comparison with the renormalized molecular levels in Table I). We want to point out that the positions of the conductance peaks in the G-V_g curve do not coincide with the renormalized molecular levels exactly proportionally, since the strong coupling between the cluster and electrodes has a very strong and complicated effect on the broadening and shift of the energy levels of the central cluster under different gate voltages with such a small distance between the cluster and the electrodes. Therefore the cooperation of the strong coupling and the gate voltage makes the equilibrium conductance curve highly asymmetric and irregular with the variation of the gate voltage. In fact, with a much longer distance, when the device works in the tunneling regime, a more symmetric and regular correspondence between the conductance peaks of the G-V_g curve and the molecular levels is expected. In our case, it is advisable to analyze the changes of the equilibrium conductance by the PDOS (partial density of states) of the central cluster at the Fermi level. The comparison of the conductance and PDOS is shown in Fig. 4. Although the conductance does not follow the change of the PDOS proportionally, it is found that the positions of the peaks and valleys in the conductance are the same as those in the PDOS, i.e., they share the common variation trends. As a conclusion, to some extent, the shift and broadening of the molecular level of the cluster induced by the gate voltage changes the PDOS at the Fermi level and eventually causes the variation of the equilibrium conductance. In the studied case, without gate voltages, the equilibrium conductance is 1.57 G_0. In the range of gate voltages that we are interested in, the conductance varies from 0.2 to 2.3 G_0. Consequently, the conductance through such an Au_{32} cluster is modulated significantly by a gate potential, producing a field-induced molecular switch behavior.

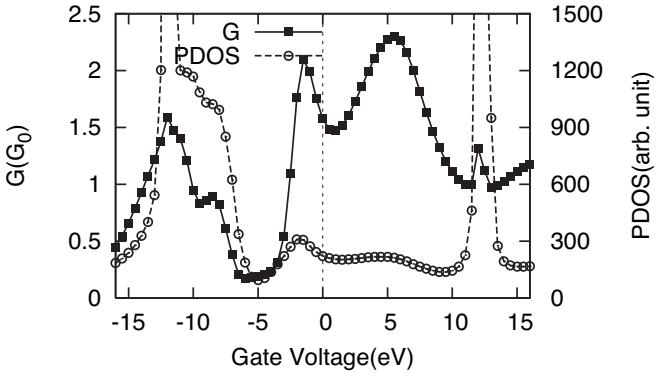

FIG. 4. The comparison of the equilibrium conductance (G) and the PDOS at the Fermi level under different gate voltages.

B. *I-V* characteristics

From the equilibrium conductance, we can only know the transport properties of the system in an equilibrium state. The I-V characteristics need to be examined when the system is out of equilibrium with a bias voltage applied to it. The current I is calculated by $I(V_b)=\int_{\mu_R}^{\mu_L}T(E,V_b)[f(E-\mu_L)-f(E-\mu_R)]dE$, where $T(E,V_b)$ is the transmission function, $f(E-\mu_{L,R})$ is the Fermi-Dirac distribution of the electrons in the electrodes, $\mu_L(V_b)=\mu_L(0)+\frac{1}{2}eV_b$ and $\mu_R(V_b)=\mu_R(0)-\frac{1}{2}eV_b$ are the chemical potentials of the left and right electrodes, with $\mu_{L,R}(0)$ the average Fermi level of the system without bias and $V_b=(\mu_L-\mu_R)/e$ the bias voltage.

In the following, by taking Fig. 1 as a model structure, the I-V characteristics with different cluster-electrode distance are studied. Four cases with $d_1=0.875$ Å, $d_2=1.775$ Å, $d_3=2.475$ Å, and $d_4=2.875$ Å are considered, where d_1 and d_2 are two shorter distances taken from the left side of the conductance peak in Fig. 2, while d_3 and d_4 are two longer distances taken from the right side of the peak. The corresponding I-V curves are presented in Fig. 5. From these graphs, we see that a high nonlinearity of the I-V curve exists in all these cases. In fact, the nonlinear response of the current to voltage is a common feature of molecular conductors.

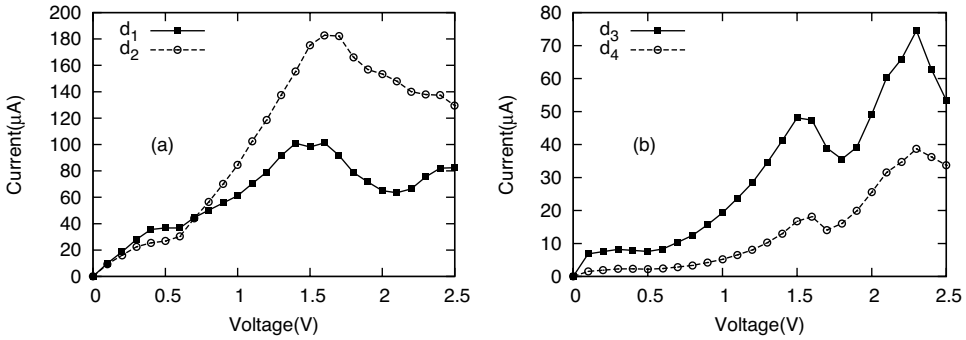

FIG. 5. *I-V* curves with the distances as: (a) d_1=0.875 Å and d_2=1.775 Å, (b) d_3=2.475 Å and d_4=2.875 Å.

All the *I-V* curves are almost completely symmetric in the positive and the negative (not shown in the figure) bias regions due to the symmetrical structure of the system along the z direction. The striking feature of the *I-V* curve is that, both in the positive and the negative bias regions, it starts by a slowly increasing section followed by a rapidly increasing section at ±0.6 V and then a NDR region indicated by the decreasing current with the increasing bias at ±1.6 V. Such a striking behavior can be explained by the nonequilibrium transmission $T(E,V_b)$ under various external biases. By taking the 1.775 Å case as an example, focusing on the positive bias part, the transmission spectra as the function of the incident electron energy and the bias voltage are presented in Fig. 6. The two green lines indicate the bias windows, i.e., the part of the transmission function in the bias window is integrated to obtain the current. In the equilibrium situation (with V_b=0 V), above and under the Fermi level, there are two energy regions $[-1.65\ \text{eV}, -0.65\ \text{eV}]$ and $[-0.05\ \text{eV}, 1.65\ \text{eV}]$ which contribute significantly to the transmission. These two regions originate from the cooperation of the incident states in the electrodes and the molecular orbitals of the cluster. Therefore, the transmission reflects the strength of the coupling between the cluster and electrodes. The first region mainly comes from the electrodes and the HOMO of the cluster and we may call it a HOMO-transmission region. The second region mainly comes from the electrodes and the LUMO of the cluster, so we may call it a LUMO-transmission region. Between these two regions, there is a gap region $[-0.65\ \text{eV}, -0.05\ \text{eV}]$ in which the transmission is very weak. Corresponding to these transmission regions, although the band structure of the electrodes is continuous (with no band gap), subject to the filtering effects of the central cluster,[31] both in the left electrode and in the right electrode, two significant energy regions in which incident electrons can go from one electrode to the other electrode are formed: one is the region $[-1.65\ \text{eV}, -0.65\ \text{eV}]$ formed by the filtering of the HOMO of the cluster and the other is the region $[-0.05\ \text{eV}, 1.65\ \text{eV}]$ formed by the filtering of the LUMO. We may call these two energy regions HFER (HOMO filtered energy region) and LFER (LUMO filtered energy region) and they are indicated as "H" and "L" in Fig. 7, respectively. The HOMO-(LUMO-) transmission regions mentioned earlier are due to the transmission of electrons from the HFER(LFER) in one electrode to the HFER(LFER) in the other.

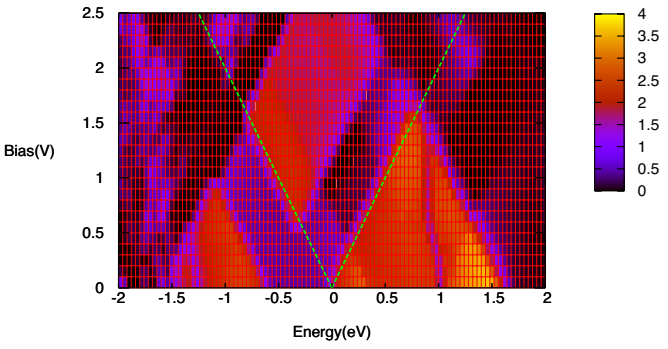

FIG. 6. (Color online) Nonequilibrium transmission spectra under various external biases with the 1.775 Å case. The two green lines indicate the bias window. The vertical color coding bar is for the values of transmission. The orange (bright) and black (dark) colors represent high and low transmission regions, respectively. The energy is relative to the average Fermi level.

The evolution of the transmission as a function of the bias voltage in Fig. 6 and subsequently the *I-V* curve can be elucidated by a rigid shift model of the two regions (the HFER and the LFER) in the electrodes under various external bias (see Fig. 7). The electron at a certain energy with a significant transmission in one electrode can only enter a state with

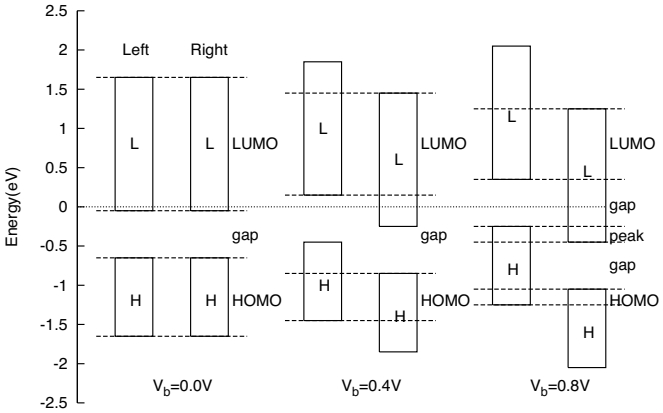

FIG. 7. The relative shift of the HFER, LFER, and gap regions in the left and right electrodes under biases V_b=0.0, 0.4, and 0.8 V. H and L represent the HFER and LFER in the electrodes, respectively. The regions between the dashed lines are the HOMO- and LUMO-transmission regions in which electrons can go from one electrode to the other with a high transmission and are labeled by "HOMO" and "LUMO." A conductance peak (labeled by "peak") appears in the gap region (labeled by "gap") in the V_b=0.8 V case. The energy is relative to the average Fermi level.

the same energy and significant transmission in the other electrode. If a bias V_b is applied to the device, the bands of the left electrode will be shifted up by $\frac{1}{2}V_b$ and the bands of the right electrode will be shifted down by $\frac{1}{2}V_b$. And the HFER and LFER in the electrodes will be shifted up or down accordingly. By applying a bias voltage less than 0.6 V (note that the magnitude 0.6 is exactly the distance between the HFER and LFER in the electrodes), with the increase of the bias, the HFER and LFER in the left electrode move upward relative to those in the right electrode, i.e., the left HFER moves close to the right LFER in energy (see the V_b $=0.4$ V case of Fig. 7). However, the common region of the HFER (and LFER) of the two electrodes with the same energy range decreases because of the relative shift of the chemical potentials in the two electrodes. This means that the energy range of the HFER (LFER) in which the electrons in the left electrode can enter the HFER (LFER) in the right electrode becomes smaller. Therefore, in the transmission spectra, the HOMO- and LUMO-transmission regions become smaller (see the red or bright triangles around −1 eV and 1 eV in the transmission spectra of Fig. 6), while the gap region is broadened. The current only has a contribution from the edge of the LUMO-transmission region, thus it increases very slowly. If we apply a voltage bigger than 0.6 V, the left HFER begins to overlap with the right LFER (see, for example, the V_b=0.8 V case of Fig. 7). For this reason, the electrons in the top part of the HFER in the left electrode can enter the bottom part of the LFER with the same energy range in the right electrode now and a transmission peak appears in the gap region (see the appearance of a red region around −0.4 eV in Fig. 6). With increasing the bias, the overlap energy range of the left HFER and the right LFER increases, thus the width and height of the peak in the gap region increase. The current now has contributions both from the LUMO edge and the transmission peak in the gap region, hence, the current increases rapidly. With the further increase of the bias larger than 1.6 V (note that the magnitude 1.0 of the bias increase from 0.6 V to 1.6 V is exactly the width of the HFER), the whole HFER in the left electrode begins to completely fall into the LFER of the right electrode and the width of the peak in the gap region ceases to broaden. Since the height of this peak is getting smaller and smaller and the LUMO-transmission region also begins to disappear in the bias window, the current begins to decrease and the NDR occurs consequently.

However, with smaller distances, only one current maximum in the *I-V* curve occurs at 1.6 V [see Fig. 5(a)], while with longer distances, a second current maximum appears at 2.3 V [see Fig. 5(b)]. This happens since, with long distances, the coupling between the cluster and electrodes becomes much weaker. With the filtering of the central cluster, additional small energy regions in which electrons in one electrode can transmit to the other electrode are formed and the transmission curve evolves into more narrow transmission regions with sharp peaks. The relative shift of these regions in the two electrodes under different biases gives rise to the transmission spectra in Fig. 8. With the increase of the bias voltage, the disappearing of peak "1" in the gap region leads to the NDR at 1.6 V and the appearance of peak "2" in the gap region creates a second current maximum at 2.3 V.

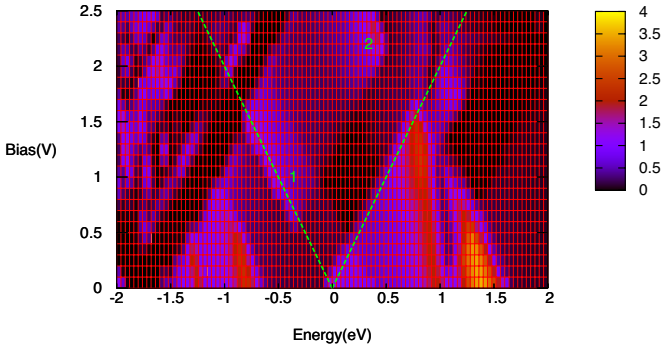

FIG. 8. (Color online) Nonequilibrium transmission spectra under various external biases with the 2.475 Å case. The two green lines indicate the bias window. The vertical color coding bar is for the values of transmission. The orange (bright) and black (dark) colors represent high and low transmission regions, respectively. The energy is relative to the average Fermi level.

IV. SUMMARY

In this work, the effects of different factors including the contact geometries and gate voltages on the equilibrium conductance and the *I-V* characteristics of an Au_{32} cluster with a cagelike structure sandwiched between two Au(100) electrodes with finite cross section have been investigated. With the variation of the distance between the cluster and the electrodes, a peak appears in the equilibrium conductance curve. However, the distance with the maximum conductance does not coincide with the equilibrium cluster-electrode distance. It means that the distance is not the only factor that determines the conductance of a molecular device. Instead, it depends on the combined effects of many factors. Our study shows that its high conductivity is caused by the mixing of the LUMO of the cluster and the electrode-induced gap state. The gate voltage affects the equilibrium conductance in an oscillatory manner and causes the variation from 0.2 to 2.3 G_0 in the case studied. The *I-V* curve, and especially, the NDR behavior in this device can be understood by a rigid shift model of the HFER and LFER in the left and right electrodes when various biases are applied.

ACKNOWLEDGMENTS

This work was supported by the National Science Foundation of China under Grants No. 10374091 and 90503005, the special Funds for Major State Basic Research Project of China (973) under Grant No. 2005CB623603, Knowledge Innovation Program of Chinese Academy of Sciences, and Director Grants of Hefei Institutes of Physical Sciences. Part of the calculations were performed at the Center for Computational Science, Hefei Institutes of Physical Sciences.

*Corresponding author. Email address: zzeng@theory.issp.ac.cn

[1] A. Aviram and M. A. Ratner, Chem. Phys. Lett. **29**, 277 (1974).
[2] M. A. Reed, C. Zhou, C. J. Muller, T. P. Burgin, and J. M. Tour, Science **278**, 252 (1997).
[3] L. Roschier, J. Penttila, M. Martin, P. Hakonen, and M. Paalanen, Appl. Phys. Lett. **75**, 728 (2001).
[4] H. Dai, Surf. Sci. **500**, 218 (2002).
[5] M. Ahlskog, P. Hakonen, M. Paalanen *et al.*, J. Low Temp. Phys. **124**, 335 (2001).
[6] P. G. Collins and P. Avouris, Sci. Am. **283**, 62 (2000).
[7] H. Kondo, H. Kino, and T. Ohno, Phys. Rev. B **71**, 115413 (2005).
[8] J. Taylor, H. Guo, and J. Wang, Phys. Rev. B **63**, 121104(R) (2001).
[9] Y. Kondo and K. Takayanagi, Science **289**, 606 (2000).
[10] Y. Oshima, A. Onga, and K. Takayanagi, Phys. Rev. Lett. **91**, 205503 (2003).
[11] Y. Oshima, H. Koizumi, K. Mouri, H. Hirayama, K. Takayanagi, and Y. Kondo, Phys. Rev. B **65**, 121401(R) (2002).
[12] J. Sha, J. J. Niu, X. Y. Ma, J. Xu, X. B. Zhang, Q. Yang, and D. R. Yang, Adv. Mater. (Weinheim, Ger.) **14**, 1219 (2002).
[13] J. Li, X. Li, H. J. Zhai, and L. S. Wang, Science **299**, 5608 (2003).
[14] M. P. Johansson, D. Sundholm, and J. Vaara, Angew. Chem., Int. Ed. **43**, 2678 (2004).
[15] X. Gu, M. Ji, S. H. Wei, and X. G. Gong, Phys. Rev. B **70**, 205401 (2004).
[16] W. Fa, J. Zhou, C. Luo, and J. Dong, Phys. Rev. B **73**, 085405 (2006).
[17] J. Taylor, H. Guo, and J. Wang, Phys. Rev. B **63**, 245407 (2001).
[18] M. Brandbyge, J.-L. Mozos, P. Ordejon, J. Taylor, and K. Stokbro, Phys. Rev. B **65**, 165401 (2002).
[19] Y. Q. Xue, S. Datta, and M. A. Ratner, Chem. Phys. **281**, 151 (2002).
[20] J. M. Soler, E. Gale, J. D. Gale *et al.*, J. Phys.: Condens. Matter **14**, 2745 (2002).
[21] B. Larade, J. Taylor, Q. R. Zheng, H. Mehrez, P. Pomorski, and H. Guo, Phys. Rev. B **64**, 195402 (2001).
[22] B. Wang, Y. Xing, L. Wan, Y. Wei, and J. Wang, Phys. Rev. B **71**, 233406 (2005).
[23] Z. X. Dai, X. H. Zheng, X. Q. Shi, and Z. Zeng, Phys. Rev. B **72**, 205408 (2005).
[24] S.-H. Ke, H. U. Baranger, and W. Yang, Phys. Rev. B **71**, 113401 (2005).
[25] In fact, the cluster structure was seldom relaxed when different biases were applied in the literature.
[26] *Science of Fullerenes and Carbon Nanotubes*, edited by M. S. Dresselhaus, G. Dresselhaus, and P. C. Eklund (Academic Press, New York, 1996).
[27] M. E. Lin, R. P. Andres, R. Reifenberger, and D. R. Huffman, Phys. Rev. B **47**, 7546 (1993).
[28] Y. Xue and M. A. Ratner, Phys. Rev. B **68**, 115406 (2003); **68**, 115407 (2003).
[29] F. Triozon, P. Lambin, and S. Roche, Nanotechnology **16**, 230 (2005).
[30] C. Joachim, J. K. Gimzewski, R. R. Schlittler, and C. Chavy, Phys. Rev. Lett. **74**, 2102 (1995).
[31] C.-C. Kaun, H. Guo, P. Grütter, and R. B. Lennox, Phys. Rev. B **70**, 195309 (2004).